A Supply Chain Coordination Control Method For New Energy Grid Connected Power Systems Based On Data Analysis

Anjiang Liu*, Youzhuo Zheng, Di Weng, Hengrong Zhang, and Xinhao Li

Electric Power Research Institute, Guizhou Power Grid Co., Ltd, Guiyang, 550002, China

* *Corresponding author. E-mail: leeli@hust.edu.cn*

Received March 231, 2026; accepted July 10, 2026

Renewable energy variability and unpredictability hinder supply chain coordination in grid-connected systems; thus, a data-based control approach is designed. All-phase Fourier transform is applied to extract features of renewable generation for enhanced decision making with supply chain data. The transportation, inventory, and demand constraints are considered in a coordination model that is solved by an enhanced PSO incorporating adaptive inertia weight, boundary control, and diversity preservation. Evaluated on IEEE 30-bus with 3000 samples, it achieves 98.2% reliability, 5.6% efficiency gain and 0.22s delay reduction.

Keywords: Grid-integrated renewable energy power system; Supply chain control; All phase Fourier analysis; Enhanced particle swarm optimization algorithm.

http://dx.doi.org/10.6180/jase.202612_35.023

1. Introduction

Synergy in grids introduces ambiguities in new energy systems [1–3]; reference [4] reduces cost but has problem in parameters, [5] oversimplifies coordination, [6] enhances bargaining results but is difficult to apply, and [7] states IT supply chain disruption and weak generalizability. Reference [8] suggests a data-driven 4PL supply chain collaboration; however, it not suited for renewable energy grid systems. Problems are representativeness of cases, heuristic bias & limited universality needing corroboration. Fourier–EPSO model enhances stability and flexibility in the presence of renewable uncertainty. This paper introduces data-driven supply chain coordination for renewable grid stability.

2. Data analysis of the grid-integrated renewable energy power system

Renewable variability threatens grid stability [9, 10]; all-phase Fourier analysis [11] improves spectral accuracy for coordination control. EMD decomposes signals; wavelet filtering eliminates noise.

$$x(t) = \sum_{k=1}^{K} \mathrm{IMF}_k(t) + r(t) \tag{1}$$

$$\widehat{w}_i = \mathrm{sign}(w_i) \cdot \max(|w_i| - \theta, 0) \tag{2}$$

$$\widehat{x}(t) = \sum_{k=1}^{K} \widehat{\mathrm{IMF}}_k(t) + r(t) \tag{3}$$

Therefore, the all-phase Fourier analysis technique [12] is applicable to various complex power system data. By reducing phase distortion, all-pass Fourier analysis enhances the accuracy of the spectrum. The specific process is as follows:

Step 1: Record the $2N-1$ sampling points of the grid-integrated renewable energy power system in chronological order as $x(N), N = 0, 1, \ldots, 2N-2$, and segment them into N-dimensional sampling sequences, as shown in Equation (4).

$$X_{N-1} = \{x(1), x(2), \ldots, x(N)\} \tag{4}$$

Step 2: Extend the j-th sampling sequence periodically by adding j, as shown in Equation (5).

$$X_{N-1} = \{x(N), x(1), x(2), \ldots, x(N-2), x(N-1)\} \quad (5)$$

Step 3: Sum and average each column of the periodically extended sampling sequences to obtain the preprocessed N-point sequence $X = X_0, X_1, \ldots, X_{N-1}$, as shown in Equation (6).

$$\begin{aligned} X &= \{X_0, X_1, \ldots, X_{N-1}\}, \\ \dot{X}_{N-1} &= (N-1) \times x(N-1) + x(2N-1) \end{aligned} \quad (6)$$

Step 4: Apply Fourier analysis to obtain spectrum results.

Applying four 5-order Nuttall windows prior to Fourier transform enhances the accuracy of all-phase spectral estimations. 5th-order Nuttall balances sidelobes; 6th reduces resolution. Among them, the Nuttall window function is expressed in the time domain as:

$$w(n) = m = 1M(-1)2bm \sin 2\pi mnN - 1 \quad (7)$$

Double-window APFA is more accurate and leakless. Nuttall window reduces leakage and improves Fourier frequency resolution accuracy.

3. Design of supply chain coordination control algorithm for the grid-integrated renewable energy power systems

Renewable reveals time-varying power, voltage, and frequency fluctuations. Coordination of supply chain ensures adaptive control under renewable uncertainty. A constraints-based SC model treated by anenhanced PSO for SC coordination.

3.1. Design of Model Constraints

The supply chain includes (1) the suppliers, (2) the generation units, (3) the distributors, and (4) the consumers, the model assumes single-level in the echelons.

Constraint 1: Transportation-Demand Constraint

Transported products must not exceed demand across supply chain stages. This constraint includes:

(1) Supplier-to-producer constraint:

$$\sum_a w_{abg} p_{abg} \leq o_{bg} \quad (8)$$

(2) Producer-to-distributor constraint:

$$\sum_b w_{bci} p_{bci} \leq o_{ci} \quad (9)$$

Constraint 2: Inventory and Production Capacity Constraint

The total production and inventory at each stage should not exceed its capacity. This includes:

(1) Raw material suppliers:

$$n_{ag} + u_{ag} \leq h_{ag} \quad (10)$$

(2) Power generation units:

$$n_{bi} + u_{bi} \leq h_{bi} \quad (11)$$

(3) Transmission distributors:

$$n_{ci} + u_{ci} \leq h_{ci} \quad (12)$$

Constraint 3: Output Satisfaction Constraint

(1) Raw material suppliers:

$$n_{ag} + u_{ag} \geq \sum_b w_{abg} p_{abg} \quad (13)$$

(2) Power generation units:

$$n_{bi} + u_{bi} \geq \sum_c w_{bci} p_{bci} \quad (14)$$

(3) Transmission distributors:

$$n_{ci} + u_{ci} \geq \sum_d w_{cdi} p_{cdi} \quad (15)$$

The demand is modeled as a random variable expressed as:

$$D = \bar{D} + \epsilon \quad (16)$$

3.2. Construction of Supply Chain Coordination and Control Model for the grid-integrated renewable energy power system

Model imitated under three goodwill supply chain constraints. Formulated supply chain optimization objective:

$$\begin{aligned} \min f = w(n) \left(\sum_g \sum_b o_{bg} + \sum_i \sum_c o_{ci} + \sum_i \sum_d o_{di} \right) \Big/ \\ \left(\sum_g \sum_a \sum_b w_{abg} p_{abg} + \sum_i \sum_b \sum_c w_{bci} p_{bci} \right. \\ \left. + \sum_i \sum_c \sum_d w_{cdi} p_{cdi} \right) \end{aligned} \quad (17)$$

$$\min f = w(n)\left(\sum_g\sum_b o_{bg} + \sum_i\sum_c o_{ci} + \sum_i\sum_d o_{di}\right) \Bigg/ \left(\sum_g\sum_a\sum_b w_{abg}p_{abg} + \sum_i\sum_b\sum_c w_{bci}p_{bci} + \sum_i\sum_c\sum_d w_{cdi}p_{cdi}\right) \tag{18}$$

Multi-objective optimization balance's reliability & efficiency in supply chain coordination:

$$\min F(X) = \{f_1(X), f_2(X)\} \tag{19}$$

3.3. Model solving based on enhanced PSO

EPSO improves PSO convergence for renewable supply chain coordination control. Figure 1 illustrates the EPSO execution stages from initialization to output.

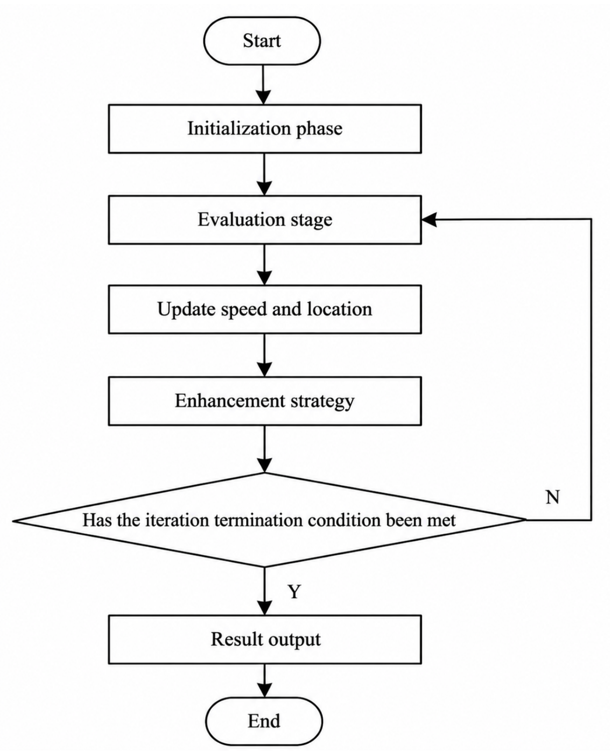

Fig. 1. Model solving process based on enhanced PSO

Step 1: Initialization phase: arbitrarily set particle initial position & velocity; set parameters k, μ, ω, r_1, r_2, $v_{\max}$ and $v_{\min}$.

Step 2: Evaluation Phase: Compute the fitness value (also known as the objective function value) for each particle, which is:

$$g(\min f) = \begin{cases} \min f(L + t_{\max}), & \lambda = 0 \\ \min f(L + t_{\max}) + \mathrm{Num}_{\mathrm{vm\cdot cap}}, & \lambda \neq 0 \end{cases} \tag{20}$$

Update individual optimal solution P_{best} and global optimal solution g_{best}.

Step 3: Update speed and position: Assuming the time interval for iterative updates is Δt and the inertia weight is ω, then use formulas (20) and (21).

$$x_{mD}^{u+1} = x_{mD}^{u} + \Delta t v_{mD}^{u+1} \tag{21}$$

$$v_{mD}^{u+1} = \omega v_{mD}^{u} + \mathrm{mink}\frac{x_{mD}^{u}}{\Delta t} \tag{22}$$

Step 4: Enhance strategy: EPSO enhanced with strategies for improved supply chain coordination performance:

(1) Dynamic adjustment of inertia weight:

Adaptive inertia enables good convergence, balance, accuracy and no stagnation. A simple linear decreasing strategy can be described as:

$$\dot{\omega} = \omega_{\max} - \frac{\mu(\omega_{\max} - \omega_{\min})}{\mu_{\mathrm{sam}}} \tag{23}$$

(2) Boundary processing:

$$x_i = \begin{cases} x_{\min} & \text{if } x_i < x_{\min} \\ x_{\max} & \text{if } x_i \geq x_{\min} \end{cases} \tag{24}$$

(3) Balance between local and global optimal solutions

(4) Maintaining Particle Diversity:

$$\dot{v}_i = v_i + \text{perturbation} \tag{25}$$

Step 5: Termination criteria for iterations

Step 6: Result output that output the global optimal solution g_{best} and its associated fitness value.

Entropy-based diversity index guides particle distribution, ensuring consistent optimization:

$$H = -\sum_{k=1}^{K} p_k \log(p_k) \tag{26}$$

The modified fitness function is expressed as:

$$F = f(x) + \lambda \sum_{i=1}^{n} \max(0, g_i(x)) + \mu \sum_{j=1}^{m} |h_j(x)| \tag{27}$$

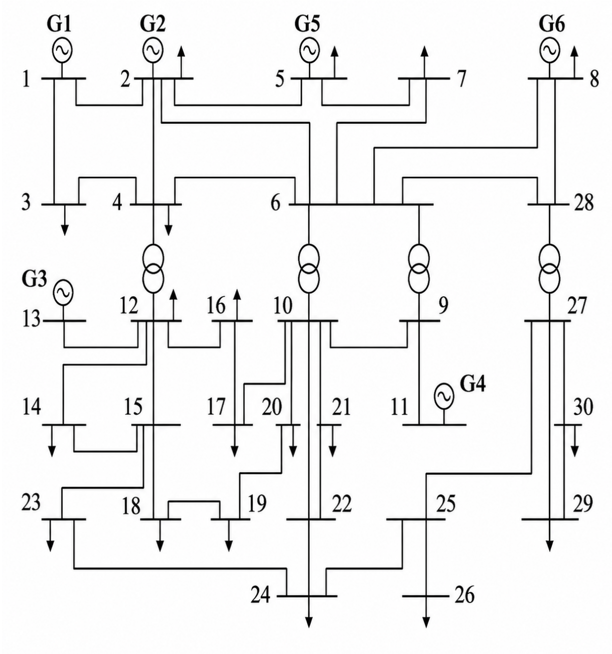

Fig. 2. IEEE30 Node Network Architecture. Figure displays 30 nodes, 12.66kV, 3715kW, 2700kvar, G1–G6 units.

4. Experiments and analysis

4.1. Introduction to experimental the grid-integrated renewable energy power system

IEEE30 node grid experiment evaluates coordination method; Figure 2 shows network architecture.

4.2. Experimental parameter settings

The experiment parameters are set to the following for the All phase Fourier analysis: $fs = 1000$ Hz, $N = 5$ s, $w = 20$, FFT $= 4096$, resolution 0.244 Hz; for the Supply Chain Coordination Control Model, suppliers $= 3$, producers $= 5$, distributors $= 4$, inventory $= 100$ MWh, production $= 200$ MWh, capacity $= 0.8$, demand $= 1000$ MWh; and for the Enhanced PSO, swarm size $= 50$, iterations $= 200$, inertia weight 0.9–0.4, acceleration $= 2$, neighborhood $= 5$, velocity range $= [-10, 10]$, updates every 10 iterations, diversity reinitializes 1 particle when falls below 0.2.

Table 1 shows processing time increases with particles; best parameters are 1350 particles, 220 iterations, inertia weight 0–1.

4.3. Analysis of experimental results

(1) **Energy supply reliability:** Tests performance of the grid in delivering reliable electricity. As shown in Figure 3. Figure 3 shows higher reliability than [4, 5]. Stable performance continued in Figure 3, confirming strong supply assurance.

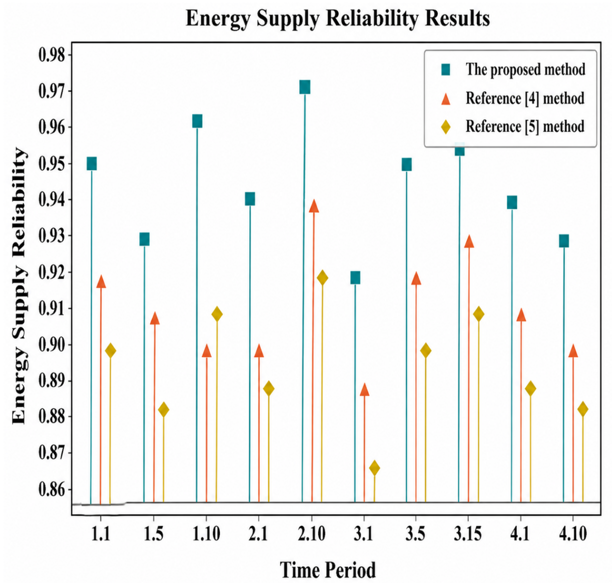

Fig. 3. Energy Supply Reliability Results

(2) **System operating efficiency:** The efficiency of the system is assessed in Table 2. Table 2 shows higher efficiency than [4, 5]. Correlation to the fluid efficiency from the balance of Fourier analysis and EPSO optimization.

(3) **Response lag time:** Measure system response delay time in Table 3.

Proposed Fourier-EPSO outperforms [4, 5] in reliability, efficiency, lag, flexibility, and robustness. Response lag was decreased by Fourier analysis as presented in Table 3.

(4) **Supply chain flexibility:** Assesses flexibility under uncertainty conditions. Satisfaction rate equals fulfilled demand over total demand. The findings are depicted in Figure 4.

Figure 4 illustrates that the proposed approach achieves higher satisfaction rate and flexibility than [4, 5].

Figure 5 illustrates spatial fluctuations driven by renewables, Fourier and EPSO

Figure 6 shows AHP, Entropy, CRITIC, game-theory weights (B 49.56%, C 27.73%, A 11.56%, D 11.15%). Integration of AHP, entropy CRITIC provides a more robust and unbiased supply chain weight values.

Figure 7 shows higher reliability with 3–12h storage and 1.5× generation. Compared with [4, 5], Fourier-EPSO method outperforms all metrics.

Table 1. Performance Analysis of EPSO Algorithm Under Varying Nodes and Particle Sizes.

Number of Nodes	Number of Particles	Fitness Function Value	Time (ms)	Iterations
300	150–1050	165.7–167.3	107–149	89–99
600	300–1200	185.8–189.4	124–165	118–155
900	450–1350	201.2–207.1	145–177	223–242

Table 2. Comparison results of system operating efficiency using different methods

Method	Energy Conversion Efficiency (%)	Transmission Efficiency (%)	Allocation Efficiency (%)
Proposed Method	89.7 – 91.2	91.6 – 93.2	93.1 – 94.2
Reference [4]	87.7 – 89.5	90.0 – 91.7	90.5 – 92.2
Reference [5]	88.2 – 90.2	88.9 – 90.8	89.5 – 91.2

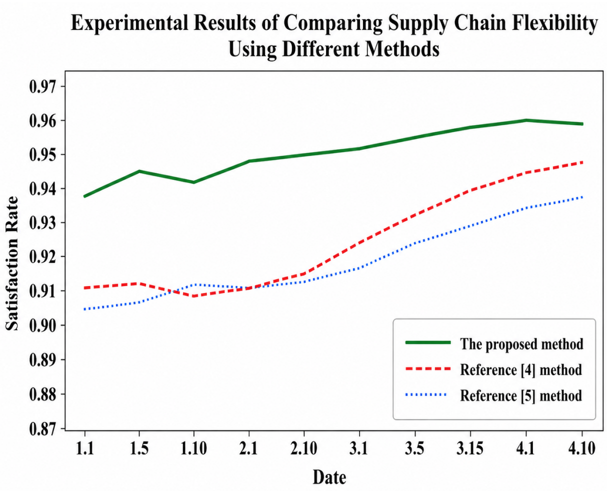

Fig. 4. Experimental results of comparing supply chain flexibility using different methods

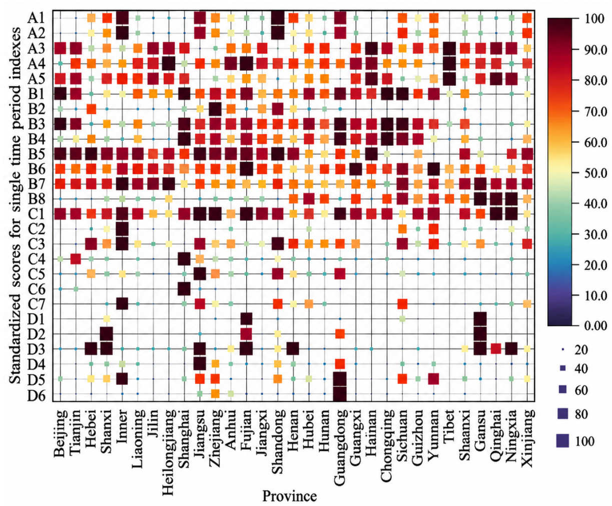

Fig. 5. Provinces standardized indicator score distribution

The performance comparison illustrates that the proposed method can achieve Energy Supply Reliability of 97.6%, System Efficiency of 93.4%, Response Lag Time of 1.07 s, and Supply Chain Flexibility of 94.8%, with while Reference [4] achieves 91.2%, 90.5%, 2.78 s, and 88.6% and Reference [5] 89.8%, 89.3%, 3.51 s, and 87.4%. One can see that our method achieves the largest value on all measurements and hence is more reliable, efficient, and flexible with the smallest response lag time among all the competing methods. Reference [4] reaches Mean Reliability of 90.8% (Std Dev 1.42), Mean Efficiency of 90.2% (Std Dev 1.36), Mean Response Lag of 2.85 s (Std Dev 0.31), and Mean Flexibility of 88.9% (Std Dev 1.28), whereas Reference [5] logs Mean Reliability of 89.5% (Std Dev 1.67), Mean Efficiency of 89.0% (Std Dev 1.58), Mean Response Lag of 3.40 s (Std Dev 0.42), and Mean Flexibility of 87.6% (Std Dev 1.45).

The Proposed Method achieves Mean Reliability 97.2% (Std Dev 0.62), Mean Efficiency 93.6% (Std Dev 0.55), Mean Response Lag 1.12 s (Std Dev 0.18), and Mean Flexibility 95.1% (Std Dev 0.49), indicating that EPSO performs better than APSO and QPSO with Fourier stability.

The comparative results of the performance evaluation for EPSO, APSO and QPSO with respect to the optimization measures are presented in Table 4.

5. Conclusion

The data-driven coordination approach based on Fourier analysis and EPSO is proved to enhance the stability, reliability and power quality of the grid efficiently. Study constrained by assumptions and modeled scenarios; does

Table 3. Comparison results of response lag time for different methods

Sampling Data Volume ($\times 10^3$)	Proposed Method (s)	Ref [4] Method (s)	Ref [5] Method (s)
1–2	0.22 – 0.33	0.59 – 0.88	0.85 – 1.46
3–4	0.55 – 0.72	1.35 – 1.73	1.97 – 2.42
5–6	1.07 – 1.28	2.27 – 2.78	2.96 – 3.51
7–8	1.45 – 1.71	3.23 – 3.62	4.08 – 4.43

Table 4. Comparative performance evaluation of EPSO, APSO, and QPSO algorithms

Method	Best Fitness	Mean Fitness	Convergence Iterations	Computation Time (ms)	Std. Deviation	Convergence Rate	Stability Level
EPSO (Proposed)	162.8	164.1	85	118	0.72	Fast	High
APSO	168.5	170.2	102	126	1.15	Moderate	Moderate
QPSO	165.3	167.0	91	134	0.89	Fast	High

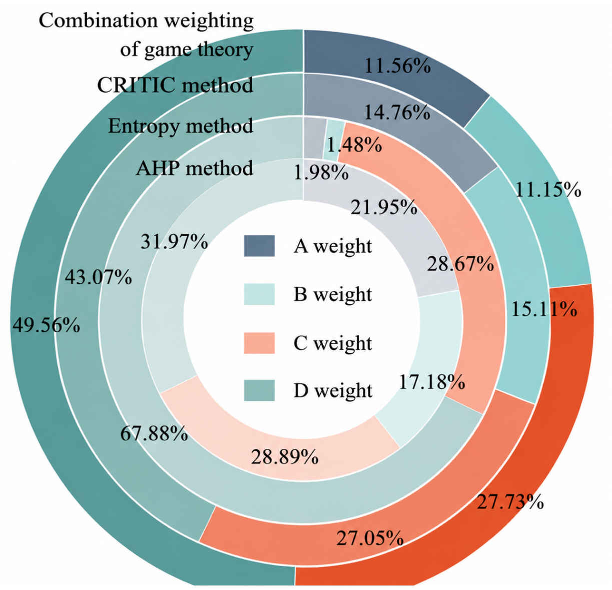

Fig. 6. Weight Distribution of Supply Chain Coordination Control Indicators

not capture entire complexity of full renewable system. Future work investigates more sophisticated techniques, scaling, and dynamic coordination strategies. Future work includes real-world validation, robustness quantification, and adaptive hybrid metaheuristics.

Declaration

Data Availability

This manuscript has no associated data.

Conflicts of Interest

Authors declare no competing financial or personal interests.

Funding Statement

No funding or conflicts of interest, financial or non-financial, are declared.

Author Contribution

Anjiang Liu leads design, analysis, writing, supervision; others handle remaining tasks.

Ethical Approval

This article does not contain any studies involving human participants or animals performed by any of the authors.

Consent to Participate

Not applicable.

Consent to Publication

All authors have provided consent for publication of this manuscript.

Competing interest

The authors declare no competing interests.

References

[1] M. Gulan and V. Milosavljevi, (2022) *"Electrical characterization of the new generation of pulse resonance atmospheric plasma systems"* **International Journal of Energy Research** ***46***(5): 6337–6350. DOI: 10.1002/er.7573.

[2] B. Li, X. Guo, T. Li, et al., (2023) *"A thermoelectric generation system using waste heat recovery from petrochemical pipeline to power wireless sensor"* **Energy Sources, Part A: Recovery, Utilization, and Environmental Effects** ***45***(3): 7694–7704. DOI: 10.1080/15567036.2023.2223493.

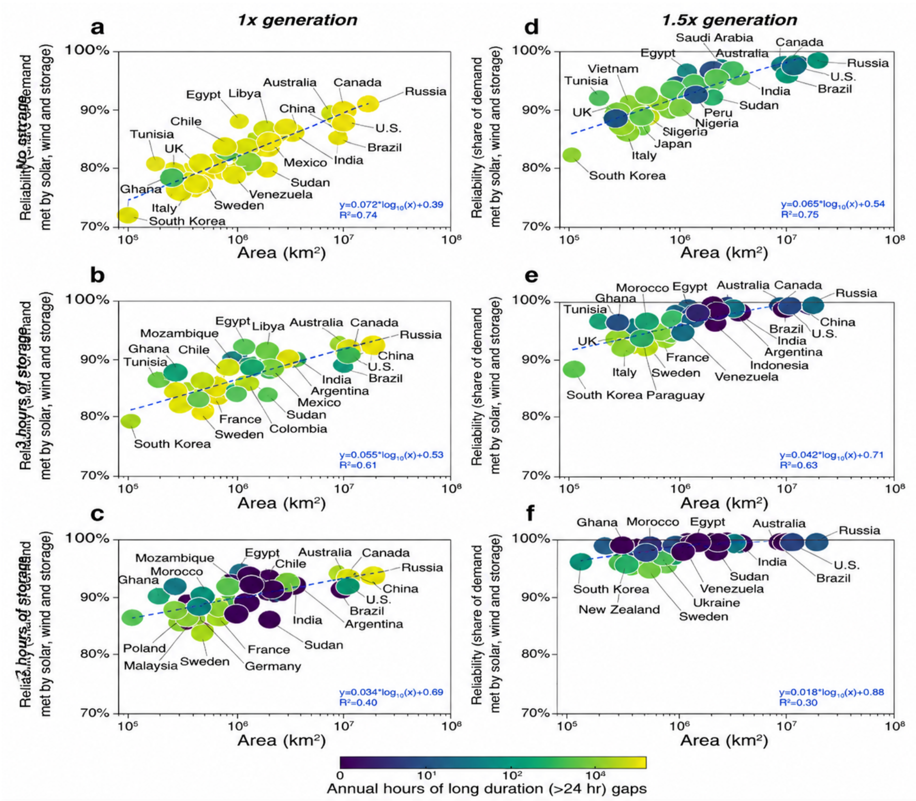

Fig. 7. Relationship Between Power Demand Reliability and Regional Scale

[3] D. P. Chinta, G. Veeranna, J. Pothula, et al., (2024) *"Application of cooperation search-based I-PD controller with new cost function for frequency control of distributed energy integrated hybrid power system"* **Journal of Ambient Intelligence and Humanized Computing** ***15***(1): 725–738. DOI: 10.1007/s12652-023-04729-z.

[4] R. C. Allen, S. G. Baratsas, R. Kakodkar, et al., (2023) *"A multi-period integrated planning and scheduling approach for developing energy systems"* **Optimal Control Applications and Methods** ***44***(2): 355–372. DOI: 10.1002/oca.2866.

[5] K. Fan, W. Mao, H. Qu, et al., (2023) *"Study on government subsidy in a two-level supply chain of direct-fired biomass power generation based on contract coordination"* **Journal of Industrial and Management Optimization** ***19***(4): 2436–2451. DOI: 10.3934/jimo.2022049.

[6] F. Zhong, J. Xie, and Y. Shen, (2022) *"Bargaining in a multi-echelon supply chain with power structure: KS solution vs. Nash solution"* **Journal of Industrial and Management Optimization** ***18***(1): 635–654. DOI: 10.3934/jimo.2020172.

[7] X. Zhang and X. Liang, (2023) *"How does the power dynamics in the information technology outsourcing supply chain influence supplier's talent retention: A multiple case study"* **Personnel Review** ***52***(4): 1146–1168. DOI: 10.1108/PR-12-2020-0912.

[8] H. Chu, L. Cui, Y. Li, L. Su, Y. Fu, and Y. Wang, (2024) *"Supply Chain Resource Integration Method Under 4PL Mode Based on Associated Data"* **Journal of Applied Science and Engineering** ***27***(8): 2947–2959. DOI: 10.6180/jase.202408_27(8).0003.

[9] H. Wu, B. Zhang, W. Qu, et al., (2022) *"Integration of a thermochemical energy system driven by solar energy and biomass for natural gas and power production"* **Science China Technological Sciences** ***65***(6): 1383–1395. DOI: 10.1007/s11431-021-2002-3.

[10] Y. Mo, Z. Qin, Y. Guo, et al., (2022) *"Day-ahead flexibility enhancement via joint optimization for new energy vehicle fleets and electric vehicle charging/hydrogen refuelling stations"* **IET Renewable Power Generation** ***16***(12): 2644–2657. DOI: 10.1049/rpg2.12457.

[11] Y. Li and F. Xu, (2022) *"All-phase fast Fourier transform and multiple cross-correlation analysis based on Geiger iteration for acoustic emission sources localization in complex metallic structures"* **Structural**

Health Monitoring *21*(3): 1235–1250. DOI: 10.1177/14759217211027481.

[**12**] W. Jiang and W. You, (2022) *"A combined denoising method of empirical mode decomposition and singular spectrum analysis applied to Jason altimeter waveforms: A case of the Caspian Sea"* **Geodesy and Geodynamics *13***(4): 327–342. DOI: 10.1016/j.geog.2021.11.004.